Inorganic Chemistry

Article

pubs.acs.org/IC

Rare-Earth Manganese Copper Pnictides $RE_2Mn_3Cu_9Pn_7$ (Pn = P, As): Quaternary Ordered Variants of the $Zr_2Fe_{12}P_7$-Type Structure

Stanislav S. Stoyko, Krishna K. Ramachandran, C. Scott Mullen, and Arthur Mar*

Department of Chemistry, University of Alberta, Edmonton, Alberta, Canada T6G 2G2

Supporting Information

ABSTRACT: The pnictides $RE_2Mn_3Cu_9Pn_7$ (Pn = P, As) have been prepared by stoichiometric reaction of the elements at 800 °C. They are quaternary ordered variants of the hexagonal $Zr_2Fe_{12}P_7$-type structure (Pearson symbol *hP*21, space group $P\bar{6}$, Z = 1; a = 9.6444(3)−9.5970(7) Å, c = 3.9027(1)−3.7761(3) Å for $RE_2Mn_3Cu_9P_7$ (RE = La−Nd, Sm, Gd−Dy); a = 9.9376(6)−9.9130(3) Å, c = 4.0194(2)−3.9611(1) Å for $RE_2Mn_3Cu_9As_7$ (RE = La−Nd)). Of the four possible sites available for the transition metal, the square pyramidal site (CN5) is occupied preferentially by Mn atoms, whereas the three tetrahedral sites (CN4) are occupied by Cu atoms. On proceeding to smaller RE members in the $RE_2Mn_3Cu_9Pn_7$ series, one of the transition-metal-centered polyhedra (Cu1) tends to become less distorted, while the remaining three (Cu2, Cu3, Mn4) become more distorted. Band structure calculations on $La_2Mn_3Cu_9P_7$ confirm that Mn−P and Cu−P contacts provide the strongest bonding interactions. Electrical resistivity measurements on $Ce_2Mn_3Cu_9P_7$ reveal metallic behavior with transitions at 165 and 18 K, probably of magnetic origin.

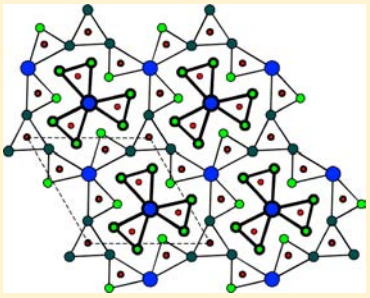

INTRODUCTION

Among ternary rare-earth transition-metal pnictides RE−M−Pn, there are numerous metal-rich phases that have a composition in which the metal-to-nonmetal ratio is close or equal to 2:1. They belong to a homologous series of hexagonal structures with the general formula $RE_{n(n-1)}M_{(n+1)(n+2)}Pn_{n(n+1)+1}$ featuring assemblies constructed from a rapidly expanding number (n^2) of triangular units as n is incremented.[1] The first four members correspond to the Fe_2P (n = 1), $Zr_2Fe_{12}P_7$ (n = 2), $Zr_6Ni_{20}P_{13}$ (n = 3), and $(La,Ce)_{12}Rh_{30}P_{21}$ (n = 4) structure types. The $Zr_2Fe_{12}P_7$ family has many representatives among phosphides $RE_2M_{12}P_7$ (M = Mn,[2] Fe,[3−5] Co,[3,6−8] Ni[3,6,9−12]) and, to a lesser extent, arsenides $RE_2M_{12}As_7$ (M = Co,[13] Ni[3,13−17]). The RE component generally spans through nearly all possible 4f substituents (apart from Pm and, curiously, La), as well as Sc and Y. Actinide representatives containing U or Th are also known.[2,18−20] The M component in these $Zr_2Fe_{12}P_7$-type phases is restricted to first-row transition metals, but there do exist a few examples containing second-row transition metals, $RE_2Rh_{12}Pn_7$ (Pn = P, As)[21] and $Eu_2Pd_{12}As_7$,[12] which adopt the closely related $Ho_2Rh_{12}As_7$-type structure. The magnetic properties measured for these compounds are diverse, with some exhibiting complicated magnetic ordering.[22−27]

A common strategy for designing new solid-state structures is to take advantage of the different sizes and coordination preferences of metals to occupy available sites. In this regard, ternary $Zr_2Fe_{12}P_7$-type pnictides serve as attractive candidates as host structures amenable to ordered substitution by more than one metal component. The $Zr_2Fe_{12}P_7$-type structure has been described in the literature in either space group $P6_3/m$ or $P\bar{6}$, with the latter now being accepted as the preferred description.[20] Of the four Fe sites (each of 3-fold multiplicity) in this structure, three of them are coordinated by pnicogen atoms in a tetrahedral geometry (CN4), whereas the fourth is coordinated in a square pyramidal geometry (CN5). Thus, in $Sc_2Fe_{12}P_7$, the Fe atoms in this CN5 site can be partially replaced with excess Sc atoms, leading to the preparation of $Sc_2(Sc_{1.6}Fe_{1.4})Fe_9P_7$ or $Sc_{3.6}Fe_{10.4}P_7$.[28] Similarly, $Yb_2(Yb_{2.6}Pd_{0.4})Pd_9P_7$ or $Yb_{4.6}Pd_{9.4}P_7$ can be regarded as being derived from a hypothetical parent compound "$Yb_2Pd_{12}P_7$" with Yb atoms partially replacing some of the Pd atoms in this site.[29] A complete substitution of Sc for Pt atoms is achieved in the silicide $Sc_2Sc_3Pt_9Si_7$ or $Sc_5Pt_9Si_7$.[30] In view of these examples which illustrate the flexibility of this structure type, it would seem possible to target the preparation of quaternary phases in which two different transition elements order within these metal sites. Following this thought, Dhahri has reported the preparation of quaternary phases $RE_2M_3M'_9Pn_7$ (RE = Gd, Er; M = Cr, W; M′ = Fe, Co; Pn = P, As), providing cell parameters but no full structure determination to confirm the metal ordering.[31]

We present here the synthesis of 12 new quaternary pnictides $RE_2Mn_3Cu_9Pn_7$ (Pn = P, As) adopting the $Zr_2Fe_{12}P_7$-type structure. Crystal structures for all members were determined to give the first definitive evidence for metal ordering within the four transition-metal sites and to enable systematic trends to be discerned. Chemical bonding was analyzed through band structure calculations on $La_2Mn_3Cu_9P_7$. Preliminary electrical resistivity measurements were made on one member, $Ce_2Mn_3Cu_9P_7$.

Received: October 25, 2012
Published: January 7, 2013

   dx.doi.org/10.1021/ic3023375 | *Inorg. Chem.* 2013, 52, 1040−1046

Table 1. Crystallographic Data for $RE_2Mn_3Cu_9Pn_7$[a]

formula	fw (amu)	a (Å)	c (Å)	V (Å^3)	ρ_c (g cm^{-3})	μ (mm^{-1})	Flack parameter	$R(F)$[b]	$R_w(F_o^2)$[c]
$La_2Mn_3Cu_9P_7$	1231.29	9.6444(3)	3.9027(1)	314.37(2)	6.504	25.24	0.44(3)	0.023	0.057
$Ce_2Mn_3Cu_9P_7$	1233.71	9.6592(3)	3.8686(1)	312.58(2)	6.554	25.83	0.49(2)	0.013	0.029
$Pr_2Mn_3Cu_9P_7$	1235.29	9.6468(4)	3.8508(2)	310.35(2)	6.610	26.54	0.76(3)	0.023	0.056
$Nd_2Mn_3Cu_9P_7$	1241.95	9.642(4)	3.8404(15)	309.2(2)	6.670	27.15	0.61(4)	0.025	0.050
$Sm_2Mn_3Cu_9P_7$	1254.17	9.6356(2)	3.8188(2)	307.05(2)	6.783	28.45	0.50(2)	0.012	0.028
$Gd_2Mn_3Cu_9P_7$	1267.97	9.5977(7)	3.7981(3)	302.99(4)	6.949	30.08	0.60(3)	0.023	0.055
$Tb_2Mn_3Cu_9P_7$	1271.31	9.6016(7)	3.7867(3)	302.33(4)	6.983	30.88	0.50(2)	0.017	0.038
$Dy_2Mn_3Cu_9P_7$	1278.47	9.5970(7)	3.7761(3)	301.19(4)	7.048	31.66	0.51(3)	0.025	0.049
$La_2Mn_3Cu_9As_7$	1538.94	9.9376(6)	4.0194(2)	343.76(3)	7.434	38.99	0.31(3)	0.024	0.051
$Ce_2Mn_3Cu_9As_7$	1541.36	9.9226(5)	3.9912(2)	340.32(3)	7.521	39.79	0.18(3)	0.022	0.047
$Pr_2Mn_3Cu_9As_7$	1542.94	9.9196(3)	3.9748(1)	338.72(2)	7.564	40.45	0.28(3)	0.019	0.047
$Nd_2Mn_3Cu_9As_7$	1549.60	9.9130(3)	3.9611(1)	337.10(2)	7.633	41.12	0.51(3)	0.022	0.054

[a]For all structures, $Z = 1$, $T = 173(2)$ K, $\lambda = 0.71073$ Å, space group $P\bar{6}$ (No. 174). [b]$R(F) = \sum||F_o| - |F_c||/\sum|F_o|$ for $F_o^2 > 2\sigma(F_o^2)$. [c]$R_w(F_o^2) = [\sum[w(F_o^2 - F_c^2)^2]/\sum wF_o^4]^{1/2}$; $w^{-1} = [\sigma^2(F_o^2) + (Ap)^2 + Bp]$, where $p = [\max(F_o^2,0) + 2F_c^2]/3$.

Table 2. Ranges of Interatomic Distances (Å) for $RE_2Mn_3Cu_9Pn_7$

compound	RE1–Pn (CN6)	RE2–Pn (CN6)	Cu1–Pn (CN4)	Cu2–Pn (CN4)	Cu3–Pn (CN4)	Mn4–Pn (CN5)
$La_2Mn_3Cu_9P_7$	3.0190(15)	2.9984(15)	2.429(2)–2.4387(14)	2.3453(8)–2.4715(14)	2.4039(12)–2.481(2)	2.488(2)–2.7419(18)
$Ce_2Mn_3Cu_9P_7$	2.9871(8)	2.9682(7)	2.4210(11)–2.4427(7)	2.3562(5)–2.4582(7)	2.4137(7)–2.4770(11)	2.5164(11)–2.7284(9)
$Pr_2Mn_3Cu_9P_7$	2.9738(16)	2.9521(15)	2.409(2)–2.4411(15)	2.3584(9)–2.4484(14)	2.4156(14)–2.474(2)	2.514(2)–2.7132(17)
$Nd_2Mn_3Cu_9P_7$	2.957(2)	2.943(2)	2.397(3)–2.4438(19)	2.3588(14)–2.4513(18)	2.4219(19)–2.472(3)	2.523(3)–2.702(2)
$Sm_2Mn_3Cu_9P_7$	2.9358(9)	2.9211(9)	2.3969(14)–2.4432(9)	2.3643(5)–2.4404(8)	2.4170(9)–2.4603(14)	2.5235(13)–2.7051(10)
$Gd_2Mn_3Cu_9P_7$	2.919(2)	2.903(2)	2.381(3)–2.438(2)	2.3574(11)–2.4275(17)	2.4113(19)–2.445(3)	2.502(3)–2.695(2)
$Tb_2Mn_3Cu_9P_7$	2.9066(14)	2.8921(14)	2.386(2)–2.4375(15)	2.3614(8)–2.4261(13)	2.4082(14)–2.442(2)	2.503(2)–2.6913(17)
$Dy_2Mn_3Cu_9P_7$	2.894(2)	2.879(2)	2.375(4)–2.435(2)	2.3614(12)–2.429(2)	2.414(2)–2.441(4)	2.506(3)–2.686(3)
$La_2Mn_3Cu_9As_7$	3.0975(7)	3.0773(7)	2.4944(15)–2.5087(9)	2.4456(12)–2.5396(9)	2.4918(9)–2.5324(14)	2.6139(18)–2.8125(14)
$Ce_2Mn_3Cu_9As_7$	3.0706(6)	3.0501(6)	2.4848(13)–2.5070(8)	2.4457(10)–2.5254(7)	2.4892(8)–2.5265(12)	2.6190(15)–2.8016(12)
$Pr_2Mn_3Cu_9As_7$	3.0542(5)	3.0349(5)	2.4827(10)–2.5062(6)	2.4453(8)–2.5218(6)	2.4901(6)–2.5252(9)	2.6235(12)–2.7969(9)
$Nd_2Mn_3Cu_9As_7$	3.0406(5)	3.0229(5)	2.4773(10)–2.5066(6)	2.4455(8)–2.5165(6)	2.4902(6)–2.5231(10)	2.6256(12)–2.7909(9)

EXPERIMENTAL SECTION

Synthesis. Starting materials were freshly filed RE pieces (99.9%, all from Hefa, except Sm, from Alfa-Aesar), Mn powder (99.6%, Alfa-Aesar), Cu powder (99.8%, Alfa-Aesar), red P powder (99.9%, Alfa-Aesar), and As lumps (99.999%, Alfa-Aesar). Stoichiometric mixtures of the elements on a 0.3-g scale were loaded into fused-silica tubes which were evacuated and sealed and then heated at 800 °C for 2 weeks. Although the title compounds were obtained in powder form after this initial heat treatment, crystal growth could be promoted by regrinding and reheating the resulting powders in the presence of about 30 mg of I_2 as a mineralizer at 800 °C for 10 days, followed by cooling to room temperature over 1 day. The products were analyzed by powder X-ray diffraction (XRD) patterns collected on an Inel diffractometer equipped with a curved position-sensitive detector (CPS 120) and a Cu Kα_1 radiation source. Generally, the title compounds constitute >80% of the product, with binary phosphides constituting the remainder. The extent of RE substitution is broader for the phosphides $RE_2Mn_3Cu_9P_7$ (RE = La–Nd, Sm, Gd–Dy) than the arsenides $RE_2Mn_3Cu_9As_7$ (RE = La–Nd). Under these synthetic conditions, extension to further RE members was unsuccessful. The compositions of needle-shaped gray crystals were determined by energy-dispersive X-ray (EDX) analysis with a Zeiss EVO MA 15 scanning electron microscope and are in good agreement with expectations (Table S1 in the Supporting Information).

Structure Determination. Suitable crystals for all $RE_2Mn_3Cu_9Pn_7$ compounds were available. Intensity data were collected on a Bruker PLATFORM diffractometer equipped with a SMART APEX II CCD area detector and a Mo Kα radiation source, using ω scans at 4–8 different ϕ angles with a frame width of 0.3° and an exposure time of 15 or 20 s per frame. The data collections were performed at low temperature (173 K) in anticipation that the reduced atomic displacements and enhanced Bragg scattering would help resolve any eventual Mn/Cu disorder and clarify the choice of space group, as discussed further below. Face-indexed numerical absorption corrections were applied. Structure refinements were carried out with use of the SHELXTL (version 6.12) program package.[32]

The problem of choosing between the centrosymmetric space group $P6_3/m$ vs the noncentrosymmetric space group $P\bar{6}$ for $Zr_2Fe_{12}P_7$-type structures has been well documented.[20] In the centrosymmetric model, pnicogen atoms are placed within 2a sites (0, 0, ±1/4), which must be half-occupied to preclude unphysically short Pn–Pn distances along the c-direction. In the noncentrosymmetric model, these sites become nonequivalent (1a (0, 0, 0); 1b (0, 0, 1/2)) so that one set can be fully occupied while the other remains empty. The centrosymmetric model thus represents an average structure, equivalent to the superposition of multiple domains of the noncentrosymmetric model. The consensus has been to refine $Zr_2Fe_{12}P_7$-type structures in $P\bar{6}$. Initial positions were taken from the structure of $Zr_2Fe_{12}P_7$ itself.[33] Atomic coordinates were standardized with use of the program STRUCTURE TIDY,[34] and atom numbering was chosen to conform to literature precedent (i.e., the four Fe atoms in $Zr_2Fe_{12}P_7$ are labeled as M1, M2, M3 in the CN4 sites and M4 in the CN5 site). Refinements were performed in which each of these four sites could be occupied by a mixture of Cu and Mn atoms. For example, in $La_2Mn_3Cu_9P_7$, the occupancies converged to 0.97(3) Cu/0.03(3) Mn in M1, 1.00(3) Cu/0.00(3) Mn in M2, 0.93(2) Cu/0.07(2) Mn in M3, and 0.09(3) Cu/0.91(2) Mn in M4, with reasonable displacement parameters for all sites. The results indicate a clear preference for Cu atoms in the CN4 sites and Mn atoms in the CN5 site, although we cannot completely discount the possibility that some Cu atoms partially disorder into the latter site. Nevertheless, the evidence seems to support strong ordering of the Cu and Mn atoms, and for simplicity we consider only this fully ordered model in the final refinements. A Flack parameter is introduced into these refinements in $P\bar{6}$ and can be interpreted as the fractional contribution of one twin component in these crystals, assumed to be racemic twins.

dx.doi.org/10.1021/ic3023375 | Inorg. Chem. 2013, 52, 1040–1046

Full crystallographic details are provided in Tables S2–S7 in the Supporting Information. They are also available in the form of crystallographic information files (CIFs) as Supporting Information or may be obtained from Fachinformationszentrum Karlsruhe, Abt. PROKA, 76344 Eggenstein-Leopoldshafen, Germany (CSD-425296 to 425307). Abbreviated crystallographic data are listed in Table 1, and selected interatomic distances are listed in Table 2.

Band Structure Calculations. Tight-binding linear muffin tin orbital band structure calculations were performed on $La_2Mn_3Cu_9P_7$ within the local density and atomic spheres approximation with use of the Stuttgart TB-LMTO-ASA program (version 4.7).[35] The basis set included La 6s/6p/5d/4f, Mn 4s/4p/3d, Cu 4s/4p/3d, and P 3s/3p/3d orbitals, with the La 6p and P 3d orbitals being downfolded. Integrations in reciprocal space were carried out with an improved tetrahedron method over 350 irreducible *k*-points within the first Brillouin zone.

Electrical Resistivity. Crystals of $Ce_2Mn_3Cu_9P_7$ were mounted for standard four-probe electrical resistivity measurements between 2 and 300 K on a Quantum Design Physical Property Measurement System (PPMS) equipped with an ac transport controller (model 7100). Silver paste (DuPont 4929N) was used as the contacting agent from the crystal to graphite fibers and gold wires. The current was 100 μA, and the frequency was 16 Hz. Measurements were repeated twice.

RESULTS AND DISCUSSION

The pnictides $RE_2Mn_3Cu_9Pn_7$ (Pn = P, As) form readily at 800 °C and are quaternary representatives of the hexagonal

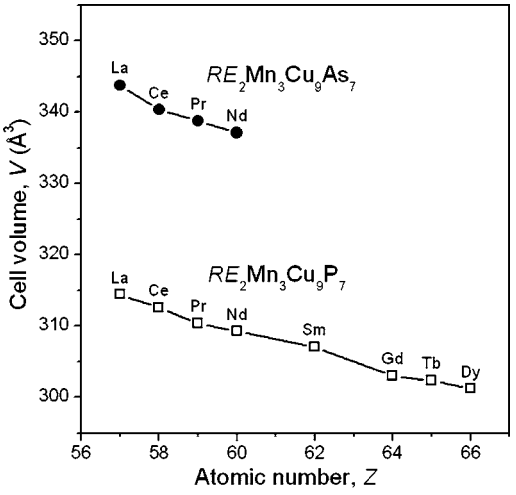

Figure 1. Plot of unit cell volumes for $RE_2Mn_3Cu_9Pn_7$ (Pn = P, As).

$Zr_2Fe_{12}P_7$-type structure.[33] The unit cell volume decreases smoothly with RE substitution, with the range extending further for the phosphides $RE_2Mn_3Cu_9P_7$ (RE = La–Nd, Sm, Gd–Dy) than the arsenides $RE_2Mn_3Cu_9As_7$ (RE = La–Nd) (Figure 1). Ternary manganese-containing phosphides $RE_2Mn_{12}P_7$ have been previously reported[2] but not the copper-containing ones "$RE_2Cu_{12}P_7$". Attempts were made to prepare other members in $RE_2(Mn_{1-x}Cu_x)_{12}P_7$ (RE = La, Nd, Tb; x = 0, 0.25, 0.50, 1.00). The existence of $RE_2Mn_{12}P_7$ (x = 0) was confirmed, but all other members of this hypothetical series, including "$RE_2Cu_{12}P_7$" (x = 1.0) could not be formed. Further attempts were made to substitute Cu with Ag, or Mn with Fe, to target the preparation of $RE_2M_3Ag_9Pn_7$ (RE = La, Nd, Tb, Ho, Lu; M = Mn, Fe; Pn = P, As), to no avail.

Like other related hexagonal structures of metal-rich phases where the metal-to-nonmetal ratio is close to 2:1,[1,36–38] the $Zr_2Fe_{12}P_7$-type structure of $RE_2Mn_3Cu_9Pn_7$ is best understood in terms of the connectivity of Pn-centered trigonal prisms

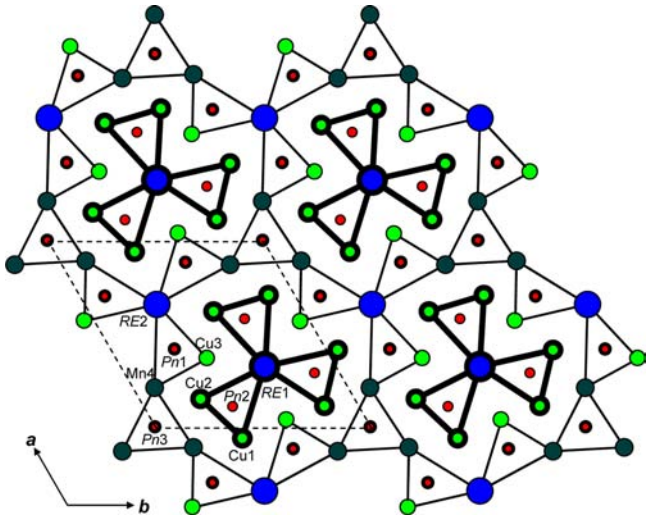

Figure 2. Structure of $RE_2Mn_3Cu_9Pn_7$ (Pn = P, As), in terms of Pn-filled trigonal prisms, viewed in projection down the *c*-axis. Thick and thin lines distinguish between atoms displaced by 1/2 the *c*-axis repeat.

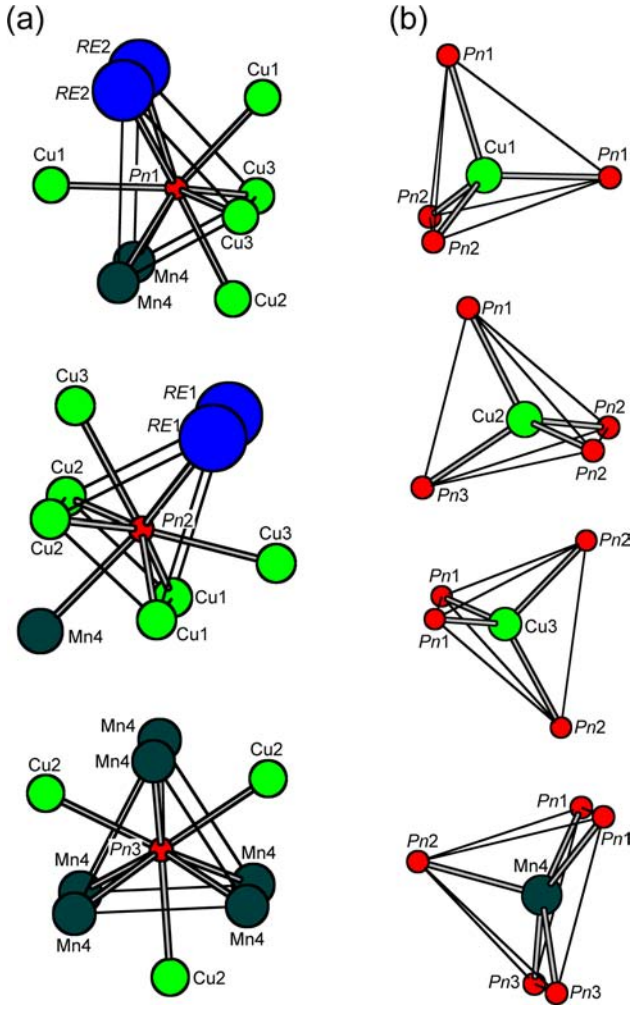

Figure 3. Coordination geometries in $RE_2Mn_3Cu_9Pn_7$ (Pn = P, As): (a) Pn atoms (CN9, tricapped trigonal prismatic). (b) Cu (CN4, tetrahedral) and Mn (CN5, square pyramidal) atoms. Viewing directions are the same as in Figure 2.

dx.doi.org/10.1021/ic3023375 | Inorg. Chem. 2013, 52, 1040–1046

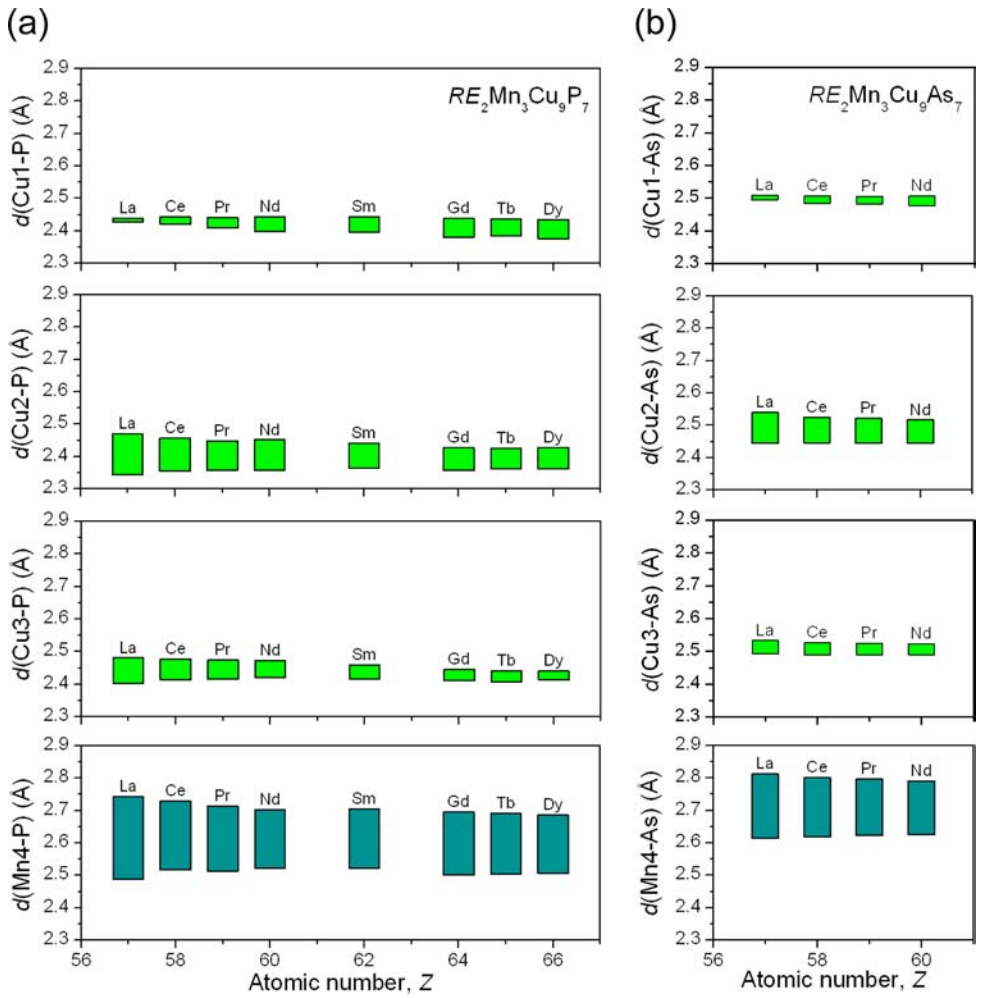

Figure 4. Ranges of Cu−Pn and Mn−Pn distances in (a) $RE_2Mn_3Cu_9P_7$ and (b) $RE_2Mn_3Cu_9As_7$ as a function of RE.

(Figure 2). All atoms in the structure are found on nets lying on the mirror planes at $z = 0$ or 1/2, which are distinguished by thick or thin rims, respectively. Trigonal prisms of each type share their triangular faces to form infinite columns aligned parallel to the *c*-direction. The Pn1- and Pn3-centered trigonal prisms each share two edges along their quadrilateral faces to form a hexagonal framework extending across the *ab*-plane. Three Pn2-centered trigonal prisms share a common edge (RE1−RE1) to form a propeller-shaped unit which lies within the large channels defined by the hexagonal framework. Additional metal atoms are found over the quadrilateral faces, so that the coordination geometry of metal atoms surrounding the Pn atoms is actually tricapped trigonal prismatic (CN9) (Figure 3a).

Alternatively, it is worthwhile to focus on the coordination of Pn atoms around the RE or transition-metal atoms. Both RE sites have trigonal prismatic coordination (CN6). The transition-metal atoms occupy four possible sites. The geometry is distorted tetrahedral (CN4) around the first three but square pyramidal (CN5) around the fourth (Figure 3b). From the structural refinements, there is a clear preference of Cu atoms for the tetrahedral and Mn atoms for the square pyramidal sites. In $Zr_2Fe_{12}P_7$-type structures, the distances to the CN5 site are generally 0.1−0.2 Å longer than to the CN4 sites, so that larger atoms should prefer the former site. However, it is not so straightforward to apply a size argument to account for the site preferences. If Pauling metallic radii are consulted, they are found to be nearly identical (Mn, 1.178 Å; Cu, 1.176 Å).[39] On the other hand, Shannon crystal radii (in which ionic bonding is assumed) tend to suggest that Mn cations are larger than Cu cations, all other things being equal (cf., Mn^{2+}, 0.80 Å (CN4), 0.89 (CN5); Cu^{2+}, 0.71 Å (CN4), 0.79 Å (CN5); Cu^{+}, 0.74 Å (CN4)).[40] Perhaps the most convincing evidence that supports the assignment of Cu vs Mn sites comes from a comparison to MnCuPn (Pn = P, As).[41] These ternary phases adopt the closely related TiNiSi-type structure, in which Cu atoms occupy tetrahedral sites and Mn atoms occupy square pyramidal sites, just as they do in the quaternary phases $RE_2Mn_3Cu_9Pn_7$. Moreover, in MnCuPn, the Mn−Pn distances (Mn−P, 2.486−2.719 Å; Mn−As, 2.585−2.793 Å) are also ∼0.2 Å longer than the Cu−Pn distances (Cu−P, 2.358−2.409 Å; Cu−As, 2.453−2.502 Å),[41] in good agreement with the values observed in $RE_2Mn_3Cu_9Pn_7$ (Table 2). Dhahri has proposed that the site preferences should be driven not by geometrical factors but rather by the need to maintain electroneutrality; that is, more electropositive and more highly charged metal atoms should prefer the higher CN site, which provides a greater number of anionic Pn atoms to satisfy the electroneutrality principle.[31] However, our inability to prepare Ag-containing analogues suggests that both size and electronegativity are important factors.

dx.doi.org/10.1021/ic3023375 | *Inorg. Chem.* 2013, 52, 1040−1046

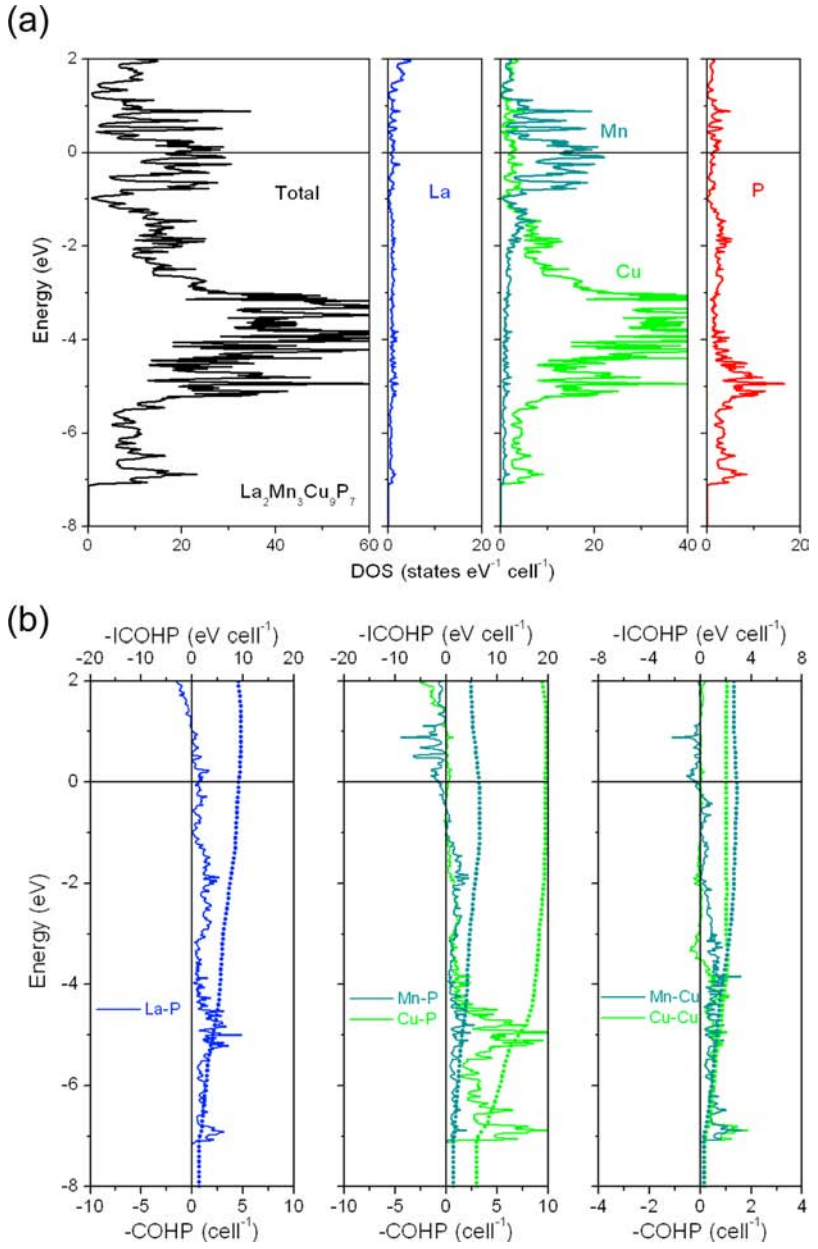

Figure 5. $La_2Mn_3Cu_9P_7$: (a) Density of states (DOS) and its atomic projections. (b) Crystal orbital Hamilton population (−COHP) curves. The Fermi level is at 0 eV.

The complete structural elucidation of all members of $RE_2Mn_3Cu_9Pn_7$ provides a good opportunity to identify systematic trends as a function of RE. As noted above, there is a clear demarcation of longer Mn−Pn and shorter Cu−Pn distances (Figure 4). Although the *average* Mn−Pn and Cu−Pn distances do not change much with RE substitution, the *ranges* of these distances, which give a measure of the degree of distortion in the coordination polyhedra, do show smooth trends. Among the three types of Cu-centered tetrahedra, the ones around Cu2 tend to be the most highly distorted. As smaller RE atoms are introduced into the structure, the distortions around Cu2, Cu3, and Mn4 become attenuated, but this is counteracted by greater distortion around Cu1. These competing trends define the limits for the largest and smallest RE atoms that can be substituted in the series.

In $Zr_2Fe_{12}P_7$-type pnictide phases, it has been speculated that metal−pnicogen bonding interactions should be the most important, followed by metal−metal bonding interactions.[20] However, to our knowledge, no electronic structure calculations have been reported previously to quantify these assertions. The electronic band structure has now been calculated for $La_2Mn_3Cu_9P_7$. Consistent with the directions of electron transfer expected from the relative electronegativities of the component elements (La, 1.1; Mn, 1.6; Cu 1.9; P, 2.2),[39] the density of states (DOS) curve reveals nearly empty La states, partly filled Mn states, mostly filled Cu states, and nearly completely filled P states below the Fermi level (Figure 5a). The Cu 3d states contribute to the wide energy manifold from −7 to −1 eV, whereas Mn 3d states contribute to the narrower one from −1 to 1 eV; both overlap with P 3p states in this region. (The P 3s states are found deeper in energy, at −12 eV.) The considerable mixing of these states leads to strong bonding interactions for Mn−P (1.28 eV/bond) and Cu−P contacts (1.62 eV/bond). The bonding is not quite optimized,

dx.doi.org/10.1021/ic3023375 | Inorg. Chem. 2013, 52, 1040−1046

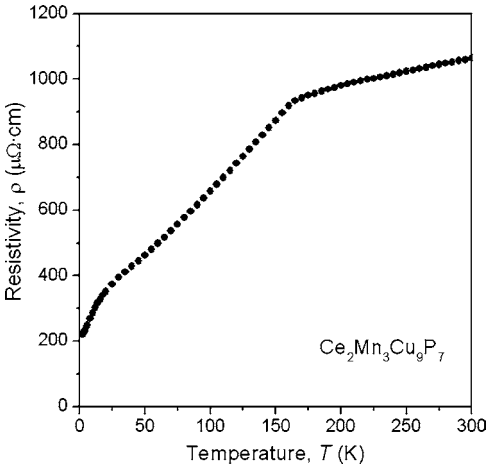

Figure 6. Plot of electrical resistivity vs temperature for $Ce_2Mn_3Cu_9P_7$.

with weakly antibonding Mn−P levels being occupied below the Fermi level and weakly bonding Cu−P levels still available above the Fermi level, as seen in the crystal orbital Hamilton population (−COHP) curves (Figure 5b). There are also less significant La−P bonding interactions (0.76 eV/bond) arising from the small mixing of La- and P-based states. If metal−metal contacts shorter than 3.0 Å are considered, they are found to be relatively weak (Mn−Cu, 0.41 eV/bond; Cu−Cu, 0.40 eV/bond).

The absence of a band gap in the DOS curve implies metallic behavior in $La_2Mn_3Cu_9P_7$. A preliminary electrical resistivity measurement on the cerium analogue $Ce_2Mn_3Cu_9P_7$ confirms this prediction (Figure 6). Although the resistivity decreases as the temperature is lowered, it undergoes two sharp transitions at 165 and 18 K, which are likely related to the onset of long-range magnetic ordering transitions. Further interpretation will have to await magnetic measurements, which requires synthetic optimization to improve sample purity.

CONCLUSIONS

The formation of the quaternary pnictides $RE_2Mn_3Cu_9Pn_7$ (Pn = P, As) illustrates that cation ordering can be achieved in $Zr_2Fe_{12}P_7$-type structures. Given that the preparation of the corresponding Ag analogues "$RE_2Mn_3Ag_9Pn_7$" fails, this ordering appears to be strictly limited to conditions in which smaller cations occupy the CN4 sites. It would be interesting to determine if higher members of the $RE_{n(n-1)}M_{(n+1)(n+2)}Pn_{n(n+1)+1}$ homologous series are also amenable to ordering if two different M components are introduced. The next member after the $Zr_2Fe_{12}P_7$-type (n = 2) is the $Zr_6Ni_{20}P_{13}$-type structure (n = 3), which contains not only square pyramidal and tetrahedral sites but also trigonal planar sites. We have attempted to synthesize "$RE_6Mn_3Cu_{17}Pn_{13}$" (RE = Nd; Pn = P, As) in which the Mn atoms would occupy the square pyramidal sites but obtained only mixtures of binary and ternary phases. Successful synthesis of these metal-rich phases may be highly sensitive to reaction conditions such as temperature, which will need to be optimized. Nevertheless, this approach of targeting phases based on the predicted compositions of hypothetical structures serves as a useful tool for solid-state synthesis.

ASSOCIATED CONTENT

Supporting Information

X-ray crystallographic files in CIF format, EDX analyses, and additional crystallographic data. This material is available free of charge via the Internet at http://pubs.acs.org.

AUTHOR INFORMATION

Corresponding Author

*E-mail: arthur.mar@ualberta.ca (A.M.).

Notes

The authors declare no competing financial interest.

ACKNOWLEDGMENTS

This work was supported by the Natural Sciences and Engineering Research Council of Canada.

REFERENCES

(1) Pivan, J.-Y.; Guérin, R.; Sergent, M. *J. Solid State Chem.* **1987**, *68*, 11−21.
(2) Jeitschko, W.; Pollmeier, P. G.; Meisen, U. *J. Alloys Compd.* **1993**, *196*, 105−109.
(3) Jeitschko, W.; Braun, D. J.; Ashcraft, R. H.; Marchand, R. *J. Solid State Chem.* **1978**, *25*, 309−313.
(4) Jeitschko, W.; Meisen, U.; Scholz, U. D. *J. Solid State Chem.* **1984**, *55*, 331−336.
(5) Oryshchyn, S. V.; Zhak, O. V.; Budnyk, S. L.; Kuz'ma, Yu. B. *Russ. J. Inorg. Chem. (Engl. Transl.)* **2002**, *47*, 1411−1414; *Zh. Neorg. Khim.* **2002**, *47*, 1541−1544.
(6) Jeitschko, W.; Jaberg, B. *Z. Anorg. Allg. Chem.* **1980**, *467*, 95−104.
(7) Jeitschko, W.; Reinbold, E. J. *Z. Naturforsch., B: Anorg. Chem., Org. Chem.* **1985**, *40*, 900−905.
(8) Budnyk, S.; Kuz'ma, Yu. B. *Pol. J. Chem.* **2002**, *76*, 1553−1558.
(9) Pivan, J. Y.; Guérin, R.; Padiou, J.; Sergent, M. *J. Less-Common Met.* **1986**, *118*, 191−200.
(10) Oryshchyn, S.; Babizhetsky, V.; Stoyko, S.; Kuz'ma, Yu. *Z. Kristallogr. − New Cryst. Struct.* **1999**, *214*, 428.
(11) Braun, T. P.; DiSalvo, F. J. *J. Alloys Compd.* **2000**, *307*, 111−113.
(12) Wurth, A.; Keimes, V.; Johrendt, D.; Mewis, A. *Z. Anorg. Allg. Chem.* **2001**, *627*, 2183−2190.
(13) Stoyko, S.; Oryshchyn, S. V. *Collect. Abstr. 9th Int. Conf. Crystal Chem. Intermet. Compd. (Lviv)* **2005**, *58*.
(14) Jeitschko, W.; Jaberg, B. *J. Less-Common Met.* **1981**, *79*, 311−314.
(15) Babizhets'ky, V.; Le Sénéchal, C.; Bauer, J.; Députier, S.; Guérin, R. *J. Alloys Compd.* **1999**, *287*, 174−180.
(16) Babizhetskyy, V.; Guérin, R.; Simon, A. *Z. Naturforsch., B: J. Chem. Sci.* **2006**, *61*, 733−740.
(17) Zelinska, M.; Zhak, O.; Oryshchyn, S.; Polianska, T.; Pivan, J.-Y. *Z. Naturforsch., B: J. Chem. Sci.* **2007**, *62*, 1143−1152.
(18) Probst, H.; Mewis, A. *Z. Anorg. Allg. Chem.* **1991**, *597*, 173−182.
(19) Stępień-Damm, J.; Kaczorowski, D.; Wochowski, K. *J. Alloys Compd.* **2001**, *315*, L4−L6.
(20) Jeitschko, W.; Meisen, U.; Albering, J. *Dalton Trans.* **2010**, *39*, 6067−6073.
(21) Pivan, J. Y.; Guérin, R.; Sergent, M. *J. Less-Common Met.* **1985**, *107*, 249−258.
(22) Reehuis, M.; Jeitschko, W. *J. Phys. Chem. Solids* **1989**, *50*, 563−569.
(23) El Ghadraoui, E. H.; Pivan, J. Y.; Peña, O.; Guérin, R.; Bonville, P. *Physica B* **1990**, *163*, 185−187.
(24) Zeppenfeld, K.; Jeitschko, W. *J. Phys. Chem. Solids* **1993**, *54*, 1527−1531.
(25) Reehuis, M.; Ouladdiaf, B.; Jeitschko, W.; Vomhof, T.; Zimmer, B.; Ressouche, E. *J. Alloys Compd.* **1997**, *261*, 1−11.
(26) Ebel, T.; Albering, J. H.; Jeitschko, W. *J. Alloys Compd.* **1998**, *266*, 71−76.

(27) Babizhetskyy, V.; Isnard, O.; Hiebl, K. *Solid State Commun.* **2007**, *142*, 80−84.
(28) Jeitschko, W.; Meisen, U.; Reinbold, E. J. *Z. Anorg. Allg. Chem.* **2012**, *638*, 770−778.
(29) Budnyk, S.; Prots, Yu.; Schmidt, M.; Schnelle, W.; Kuz'ma, Yu.; Grin, Yu. *Z. Anorg. Allg. Chem.* **2004**, *630*, 1062−1067.
(30) Lorenz, P.; Jung, W. *Z. Anorg. Allg. Chem.* **2009**, *635*, 920−925.
(31) Dhahri, E. *J. Phys.: Condens. Matter* **1996**, *8*, 4351−4360.
(32) Sheldrick, G. M. *SHELXTL*, version 6.12; Bruker AXS Inc.: Madison, WI, 2001.
(33) Ganglberger, E. *Monatsh. Chem.* **1968**, *99*, 557−565.
(34) Gelato, L. M.; Parthé, E. *J. Appl. Crystallogr.* **1987**, *20*, 139−143.
(35) Tank, R.; Jepsen, O.; Burkhardt, A.; Andersen, O. K. *TB-LMTO-ASA Program*, version 4.7; Max Planck Institut für Festkörperforschung: Stuttgart, Germany, 1998.
(36) Madar, R.; Ghetta, V.; Dhahri, E.; Chaudouet, P.; Senateur, J. P. *J. Solid State Chem.* **1987**, *66*, 73−85.
(37) Kuz'ma, Yu.; Chykhrij, S. In *Handbook on the Physics and Chemistry of Rare Earths*; Gschneidner, K. A., Jr., Eyring, L., Eds.; Elsevier: Amsterdam, The Netherlands, 1996; Vol. *23*, pp 285−434.
(38) Prots', Yu. M.; Jeitschko, W. *Inorg. Chem.* **1998**, *37*, 5431−5438.
(39) Pauling, L. *The Nature of the Chemical Bond*, 3rd ed.; Cornell University Press: Ithaca, NY, 1960.
(40) Shannon, R. D. *Acta Crystallogr., Sect. A* **1976**, *32*, 751−767.
(41) Mündelein, J.; Schuster, H.-U. *Z. Naturforsch. B: J. Chem. Sci.* **1992**, *47*, 925−928.